Journal of Nano- and Electronic Physics
Vol. **18** No 4, 04030(8pp) (2026)

Журнал нано- та електронної фізики
Том **18** № 4, 04030(8cc) (2026)

OPEN ACCESS

REGULAR ARTICLE

Rhodamine 6G and Nile Red Containing Porous Films with CdTe Quantum Dots for Highly Sensitive Detection of Acetone and Ammonia in the Air

Ya.P. Lazorenko[1,2], V.P. Mitsai[2], S.O. Mamilov[2], V.O. Sokolov[2], V.O. Golub[2,*]

[1] *G.V. Kurdyumov Institute for Metal Physics of the NAS of Ukraine, 03142 Kyiv, Ukraine*
[2] *V.G. Baryakhtar Institute of Magnetism of the NAS of Ukraine, 03142 Kyiv, Ukraine*

(Received 20 April 2026; revised manuscript received 18 August 2026; published online 21 August 2026)

Detecting molecules at low concentrations in multicomponent gas environment is a difficult task. Although various sensors are currently under research and development, they do not always meet the requirements of high sensitivity, selectivity, operation at room temperature, and low cost. One promising approach to achieving this is fluorescent film sensors. The objective of this study was to investigate the optical properties and fluorescence-based sensor responses of porous films doped with rhodamine 6G or Nile red, or their complexes with CdTe quantum dots. The film matrices consisted of polyvinyl alcohol, Aerosil (fumed silica), or ethylene vinyl acetate with silica gel. Quantum dots were introduced to enhance the fluorescence signal via non-radiative Förster resonance energy transfer. Optical absorption and fluorescence spectra of films in the visible region have been acquired. The decrease in fluorescence intensity determined the analyte content. Sensor responses to low concentrations of ammonia or acetone (5 ppm) have been detected. The highest sensitivities to acetone and ammonia were demonstrated by Aerosil doped with rhodamine 6G and polyvinyl alcohol doped with Nile red and 2.9 nm CdTe quantum dots, respectively. Such high sensitivity was observed at room temperature. Based on the experimental results and the unique properties of the materials, it was concluded that these films could be used as sensitive sensor elements for non-invasive disease diagnosis by detecting biomarker concentrations in exhaled air, or for environmental monitoring.

Keywords: Sensor, Fluorescent dyes, Rhodamine 6G, Nile red, Acetone, Ammonia, Fluorescence, Quantum dots.

DOI: 10.21272/jnep.18(4).04030

PACS numbers: 07.07.Df, 33.50.Dq, 78.20. – e, 78.67.Hc, 81.07.Ta, 87.64. – t

1. INTRODUCTION

Human exhaled air contains more than 3000 different molecules, mainly at trace concentrations [1]. Acetone and ammonia are among the most studied biomarkers. In particular, an acetone level over 1.8 ppm (parts per million) in human exhalation is observed in type 1 diabetes, heart failure, and lung cancer [2]. Ammonia excess over 1 ppm is observed in cases of liver and kidney dysfunction, and lung cancer [3].

At present, the highest sensitivity (up to ppb levels) to these gases is provided by metal-oxide sensors [4]. However, they have significant drawbacks (insufficient selectivity, sensitivity to humidity, and high operation temperature) that prevent their widespread use in diagnostics [5, 6]. An alternative to metal oxide-based sensors are optical sensors, especially those that respond by changing fluorescence parameters (intensity or spectral position). They provide high sensitivity, operation at room temperature, low cost, and ease of manufacture. Also, the physical mechanisms of sensing can provide high selectivity for the analyte [7, 8].

Encouraging results in the detection of volatile substances are demonstrated by sensors based on solid film matrices doped with organic dyes [4, 9-12]. At present, they provide sensitivity in the range of 0.2-10 ppm. These and other results suggest that the performance of sensors of this type can be further improved by varying the matrix and dopant parameters.

The enhancement of dye fluorescence by quantum dots (QDs) via Förster resonance energy transfer (FRET) is of interest, as it can be used to increase the effective fluorescence signal of the sensor film. This energy transfer between two fluorophores results from a dipole-dipole interaction between the donor and acceptor. The efficiency of this process increases with decreasing donor-acceptor distance (no more than 10 nm) and increasing overlap between the donor fluorescence and the acceptor absorption spectra. The sensor properties of hybrid structures comprising conjugates of QDs and dyes are currently under active investigation. QDs have a high fluorescence quantum yield and, unlike organic dyes, are less prone to photobleaching, thereby protecting the dye-acceptor from it [13, 14].

This work aimed to study the effect on the sensor properties of (1) the use of porous matrices and doping dyes and (2) the introduction of quantum dots.

Since rhodamine 6G (R6G) and Nile red (NR) dyes exhibit fluorescence sensitivity to the surrounding media, it is of interest to investigate them as fluorophores in films whose fluorescence is modulated upon interaction with adsorbed acetone or ammonia

* Correspondence e-mail: golub@imag.kiev.ua

© 2026 The Author(s). Journal of Nano- and Electronic Physics published by Sumy State University. This article is distributed under the terms and conditions of the Creative Commons Attribution (CC BY) license.

Cite this article as: Ya.P. Lazorenko, et al., *J. Nano- Electron. Phys.* 18 No 4, 04030 (2026) https://doi.org/10.21272/jnep.18(4).04030

molecules. The primary focus is on studying their properties in solution, including the creation of active laser media [15-18]. Still, only a few publications address gas-sensitive materials to ammonia and acetone.

The fluorescent organic dye R6G belongs to the xanthene family and is cationic, i.e., it consists of an organic cation and an inorganic anion. The π-electron transition in the organic cation determines its spectral properties. The absorption and fluorescence spectra of R6G overlap significantly and are nearly mirror-symmetric. The quantum yield is usually high, $\varphi F > 0.9$. The Stokes shift depends on the polarity of the environment and is mainly 19-28 nm [19].

NR is a neutral hydrophobic organic fluorescent dye belonging to the group of oxazine dyes. It exhibits intense fluorescence and strong solvatofluorochromic properties, which are associated with the significant dipole moment of the dye molecule in both its ground and excited states. The more polar the environment surrounding the dye molecule, the more pronounced the red shift (range exceeds 110 nm) of its absorption and fluorescence bands, and the lower the intensity of these bands. In the visible region of the spectrum, the bands are caused by transitions between π-electron orbitals with intramolecular charge transfer [20].

R6G or its derivatives are mainly studied in sensors for heavy metal ions in solutions. In particular, the presence of Al^{3+} and Hg^{2+} ions increased the dye's fluorescence intensity and altered its absorption spectrum in solution [21, 22]. Also, sensor membranes based on ethylcellulose, poly (vinyl chloride), and poly (vinyl acetate) with immobilized R6G were sensitive to dissolved ammonia in water at levels of 0.1-10 μg/ml (however, the most sensitive membranes showed a non-reversible response) [23]. At the same time, there are almost no studies on its sensor properties to acetone or ammonia in the gas phase. There are reports of a sensor sensitive to ammonia, which is formed during meat decomposition. It is based on R6G conjugated to ß-cyclodextrin and, upon interaction with NH_3 vapors, emits fluorescence in the yellow region of the spectrum [24].

NR is widely used for bioimaging due to its exceptional sensitivity to the molecular environment [25] and is being studied as a fluorescent and colorimetric probe for microplastics [26], biomembrane lipids [27], biothiols [28], and superoxide radical ions [29] in cells. There are a few studies on its sensor characteristics to acetone or ammonia in the air. Thus, a sensor based on a tapered small core singlemode fiber coated with a layer of silicate sol-gel with NR showed an optical response to volatile organic compounds – acetone, ethanol, and methanol – as a shift in the absorption band at concentrations of 40-200 ppm, with a response (to acetone) and recovery time of 5-10 minutes [30]. *Y*-type zeolites coated with NR showed similar results. However, the material's sensitivity to acetone was low [31]. A sensor based on a micellar composite of fluorescein derivative with NR showed sensitivity to ammonia, which is released when seafood decomposes. When ammonia was adsorbed in the concentration range of 0-35 ppm, the fluorescence spectrum shifted to the short-wavelength region [32].

Porous matrices based on silicon dioxide, such as silica gel or fumed silica (Aerosil), have a large specific surface area and are promising for adsorbing volatile molecules from gas environments in optical gas sensor materials. The presence of silanol groups on the surface of such sorbents gives them the ability to form Van der Waals bonds, as well as to be both donors and acceptors of hydrogen bonds. As a result, it is possible to immobilize dye molecules on the surface of pores and adsorb volatile molecules from the gaseous medium [33].

2. EXPERIMENTAL

To prepare experimental samples, Rh6G and NR dyes were used as dopants. To enhance fluorescence, two types of CdTe QD nanoparticles were embedded in ammonia sensors. Their diameters were 2.9 nm and 2.3 nm, luminescence maxima were 620 nm and 549 nm, and quantum yields were 15 % and 30 %, respectively. The nanoparticles were stabilized with the surfactant thioglycolic acid. Quantum dots with a luminescence maximum at 549 nm were intended to form donor-acceptor pairs with Rh6G molecules, and those with a maximum at 620 nm were intended to form pairs with NR molecules. Such combinations arose from the dependence of FRET efficiency on the overlap between the QDs' luminescence and the dye's absorption spectra.

Polyvinyl alcohol (PVA) and ethylene vinyl acetate (EVA) were used as polymer matrices for sensor films. Aerosil A-180 (powdery dispersed pyrogenic (fumed) silica, which consists of silicon dioxide SiO_2 nanoparticles sintered into agglomerates, characterized by high textural porosity and a specific surface area of 175 m^2/g) and silica gel-60 (mesoporous silicon dioxide SiO_2 with a granule size of 37-63 microns, a pore size of 60 Å, and a specific surface area of 500±50 m^2/g) were used as sorbents with a large specific surface area.

To prepare air mixtures containing volatile compounds, liquid acetone and a 10 % aqueous ammonia solution were used.

Three types of sensor film samples, differing in matrix material, were obtained using the following techniques.

For the first sample type, ethanol solutions of dyes R6G and NR at a concentration of 10^{-3} M (mol/L) were prepared. The solutions were mixed using a magnetic stirrer, with aqueous colloidal CdTe QD solutions stabilized with thioglycolic acid in a 1:1 ratio. Separately, a 5% aqueous solution (hydrogel) of polymer was prepared from granulated PVA. A dye-QD mixture was added to the PVA hydrogel, and glycerol was used as a plasticizer, added in a ratio of 1:50. The prepared gel was stirred with a magnetic stirrer for 120 min and then cast onto glass substrates. The hydrogel was applied to completely cover the surfaces of all substrates with a uniform film. The samples were then dehydrated at a temperature of 60-65 °C. The resulting PVA-based polymer film samples had dimensions of $7 \times 35 \pm 2$ mm and a thickness of 20 ± 5 μm, with a transparent texture (Fig. 1(a)).

For the second sample type, as in the first, mixtures of ethanol solutions of dyes R6G and NR ($C = 10^{-3}$ M) with aqueous colloidal CdTe QD solutions in a 1:1 ratio were prepared. A layer of EVA polymer was melted and applied to glass substrates heated to 80 °C. A layer of silica gel-60 was applied to the resulting molten polymer

layer. After cooling to 25 °C, the polymer hardened, and a mixture of dye with QDs was dropped onto the resulting two-layer composite. The resulting composite was dried at 25 °C. Such polymer film coatings had dimensions of $7 \times 35 \pm 2$ mm and a thickness of 80 ± 5 μm and were matte translucent (Fig. 1(b)).

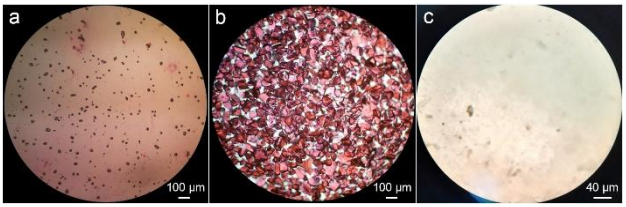

Fig. 1 – Micrographs of film samples: a – based on PVA with dye and QDs, b – based on EVA and silica gel-60 with dye and QDs, c – based on Aerosil A-180 with dye

For the third sample type, a water-ethanol suspension of A-180 Aerosil particles was first obtained. Then, this suspension was homogenized using a magnetic stirrer. Next, the suspension was dispersed using a UZDN-A ultrasonic disperser. The resulting suspension was poured into a container, which was a metal cylinder with a diameter of 51 mm and a height of 12 mm, the bottom of which was glued to a polyethylene terephthalate substrate. This container with the suspension was placed in the cell of the RS-6 centrifuge. Dispersed Aerosil particles were sedimented onto the substrate at 2600 rpm for 30 minutes. As a result, an Aerosil film formed on the substrate, which was dried at 25 °C. The film on the substrate was cut into elements measuring $7 \times 25 \pm 2$ mm, which were film samples. The film thickness was 20 ± 5 μm.

The Aerosil films were doped with dyes by drop-coating. Ethanol solutions of R6G or NR at a concentration of 10^{-4} M were applied using a liquid-dispensing micropipette. Due to capillary forces, the solution was evenly distributed throughout the film volume. The samples were dried in air at 25 °C. The resulting film samples were matte translucent (Fig. 1(c)).

The absorption and fluorescence excitation spectra of the solutions and film samples were measured using a Specord M40 UV-VIS spectrophotometer (resolving power 0.25 nm) with a fluorescence attachment. The absorption spectra of Aerosil films with immobilized R6G were recorded with a ULAB-102 spectrophotometer (repeatability 0.5 nm). The fluorescence spectra were measured on an SL 40-2 spectrometer (resolving power 0.8 nm). The fluorescence intensity of the solutions at a fixed wavelength was measured using a Flx-800T fluorometer. The fluorescence kinetics of the films and their fluorescence responses to acetone were measured using a Specord M40 UV-VIS spectrophotometer, and to ammonia using a Flx-800T fluorometer, which was modified with a gas quartz cuvette for measuring film samples under the required gas environment.

To study the sensor responses of the prepared samples to ammonia and acetone, air mixtures containing specified concentrations of these species were prepared using the static volumetric method of preparing gas mixtures [34]. A prepared gas sample with a known analyte concentration was introduced into a cuvette with a film sample using a syringe. It was also possible to recirculate 1 L (container volume) of the air mixture with the corresponding impurities through the cuvette with the sample. A 4 ml quartz cuvette was used. The sample's fluorescence response was determined by measuring the kinetics of fluorescence intensity before and after injection of the mixture. When studying the sensor properties of the created film samples, the analytical signal was defined as the change in fluorescence intensity of the sample resulting from its interaction with ammonia or acetone molecules in the gas sample.

All experiments and gas mixture preparations were carried out at room temperature (near 293 K).

3. RESULTS AND DISCUSSION

The maximum of the absorption spectrum of the ethanolic solution of R6G in the visible region was at $\lambda_{max} = 528$ nm, and a fluorescence maximum was at $\lambda_{max} = 556$ nm. The absorption maximum of NR in ethanol occurred at $\lambda_{max} = 547$ nm, and the fluorescence maximum at $\lambda_{max} = 627$ nm. The positions of the maxima agree with those reported in [20, 35]. The concentration of the solutions was 10^{-3} M.

The overlaps of the absorption spectra of the acceptor and the fluorescence spectra of the energy donor of electronic excitation are shown in Fig. 2(a) (for R6G and CdTe QDs with fluorescence maximum at $\lambda_{max} = 549$ nm) and Fig. 2(b) (for NR and CdTe QDs with fluorescence maximum at $\lambda_{max} = 620$ nm). The dyes were dissolved in ethanol, and the QDs were dissolved in water.

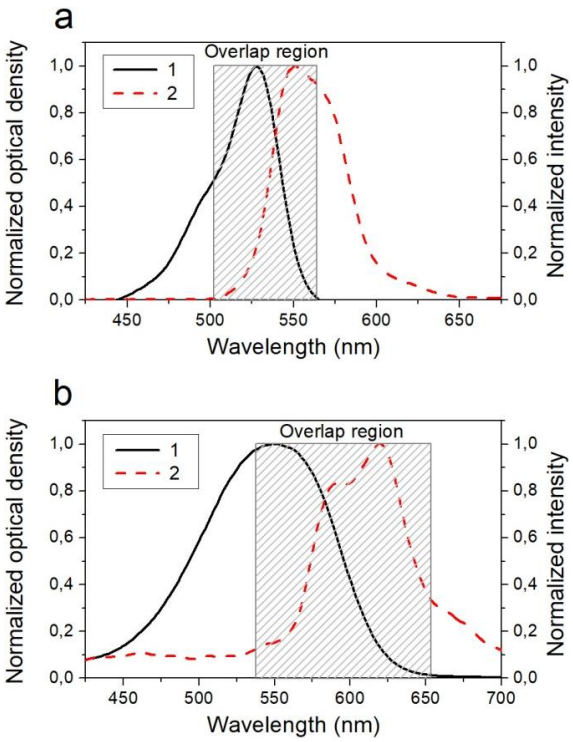

Fig. 2 – Overlaps of absorption spectrum (1) of dye (energy acceptor) with fluorescence spectrum (2) of QDs (energy donor). (a) R6G dye and CdTe QDs ($\lambda_{max} = 549$ nm), (b) NR dye and CdTe QDs ($\lambda_{max} = 620$ nm). Spectra are normalized to the maximum values

In both cases, the acceptor's absorption spectrum and the energy donor's fluorescence spectrum overlap significantly. Such overlap is a necessary condition for singlet-singlet nonradiative energy transfer. The different positions of the donor and acceptor fluorescence emission maxima allow them to be identified separately.

The relative fluorescence intensities of donor-acceptor systems, and separately of dye solutions in ethanol and CdTe QDs solutions in water, are shown in Fig. 3(a) (for R6G and CdTe QDs (λ_{max} = 549 nm)) and Fig. 3(b) (for NR and CdTe QDs (λ_{max} = 620 nm)).

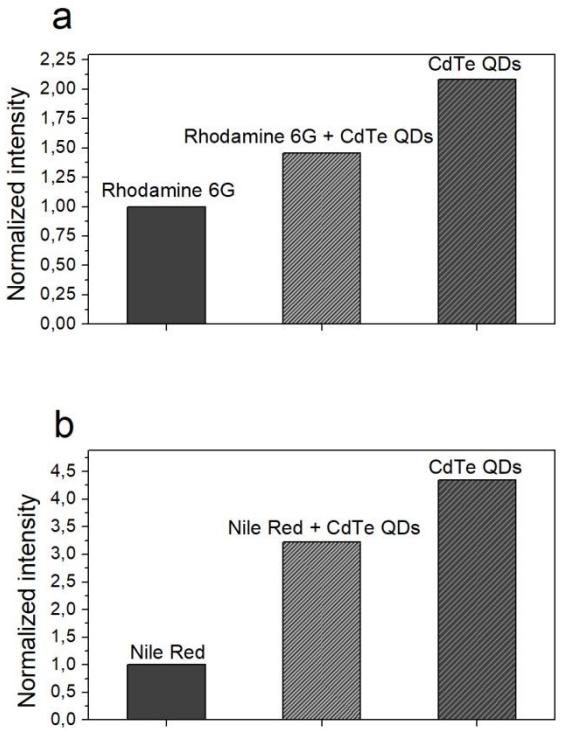

Fig. 3 – Comparison of the normalized fluorescence intensities of dye solutions, QDs, and their mixtures. (a) R6G dye and CdTe QDs (λ_{max} = 549 nm), (b) NR dye and CdTe QDs (λ_{max} = 620 nm)

As shown in the diagram in Fig. 3, the presence of a donor increases acceptor fluorescence by 1.46 times for R6G and by 3.23 times for NR, which indicates efficient nonradiative energy transfer from the singlet excited QDs.

These donor-acceptor complexes, which exhibited fluorescence enhancement, were used to synthesize film samples to amplify their fluorescence signal. As a result, the signal-to-noise ratio increased, which is essential for sensor detection. First, the spectra of the films were measured in clean air, free of impurities.

Fig. 4 shows the absorption and fluorescence spectra of film samples doped with R6G and NR dyes, normalized to the maximum band intensities. The maxima of the absorption and fluorescence spectra are given in Table 1. In films with broad, low-intensity spectral bands, the exact position of the maximum could not be determined. Therefore, the range of values for the spectral maximum is provided.

Regarding absorption spectra, a hypsochromic (toward shorter wavelengths) shift of 3 nm was observed in the PVA film with R6G/QDs compared to the dye solution. In the film with EVA and silica gel with R6G/QDs, a bathochromic (to a longer wavelength) shift of 2 nm was found. In the Aerosil film with R6G, a hypsochromic shift of 5 nm was present. Also, in the absorption spectra of these films, especially based on EVA with silica gel and PVA, there is a shoulder in the 500 nm region. For the Aerosil film with NR, the bathochromic shift compared to the ethanolic dye solution was 29 nm, for EVA and silica gel with NR/QDs was 46-63 nm, and for PVA with NR/QDs was 93-113 nm.

Regarding fluorescence spectra, a bathochromic shift by 25 nm was observed in the Aerosil film with R6G compared to ethanolic or aqueous dye solutions [36], for the EVA and silica gel film with R6G/QDs – bathochromic by 18 nm, and for the PVA film with R6G/QDs – hypsochromic by 9 nm. In all samples, a shoulder is observed in the fluorescence spectrum at 620-630 nm. In the Aerosil film with NR, the position of the band has a hypsochromic shift by 17 nm compared to the ethanolic dye solution, for the EVA and silica gel film with NR/QDs – hypsochromic by 23 nm, and for the PVA film with NR/QDs – bathochromic by 3-23 nm.

Thus, shifts in the absorption and fluorescence spectra in different film matrices indicate the sensitivity of the R6G and NR dyes to the molecular environment. The largest shifts were found for NR.

The obtained spectral absorption bands for R6G molecules in films in the visible region are caused by transitions from the S_0 ground state to the S_1 singlet state of the π-electrons. Transitions $S_1 \rightarrow S_2$ with the same absorption wavelength are also possible [15, 35]. The shoulders in the absorption spectrum at 500 nm and in the fluorescence spectrum in the 620-630 nm region may indicate both the oligomerization of dyes in the film and the influence of vibrational transitions on the electronic spectrum [35, 36]. The shape of the NR spectra in this range is also caused by singlet S_1 [37] transitions of π-electrons with intramolecular charge transfer [25, 38]. As a result of such charge transfer, the dipole moment of the dye molecule changes significantly. Its interaction with the dipole moment of the polar molecular environment determines the pronounced solvatofluorochromic properties of NR. Therefore, the position and intensity of the spectral bands depend significantly on the medium polarity. Meanwhile, the fluorescence of R6G and NR occurs during the radiative transition from the excited S_1 to the ground S_0 level. At the same time, relaxation $S_2 \rightarrow S_1$ in R6G occurs purely non-radiatively [15].

Experiments on the study the sensor responses of film samples showed that when acetone molecules are adsorbed on the surface of the Aerosil film with R6G from the air, the fluorescence intensity of the film decreases (Fig. 5). Also, when interacting with ammonia molecules, a decrease in fluorescence intensity was observed in EVA with silica gel and PVA films functionalized with R6G/QDs. This decrease occurs due to the quenching of dye fluorescence by analyte molecules. The quenching value was proportional to the concentration of acetone or ammonia in the air inside the measuring cell containing the sample. In the case of acetone, the shift of the fluorescence band was insignificant.

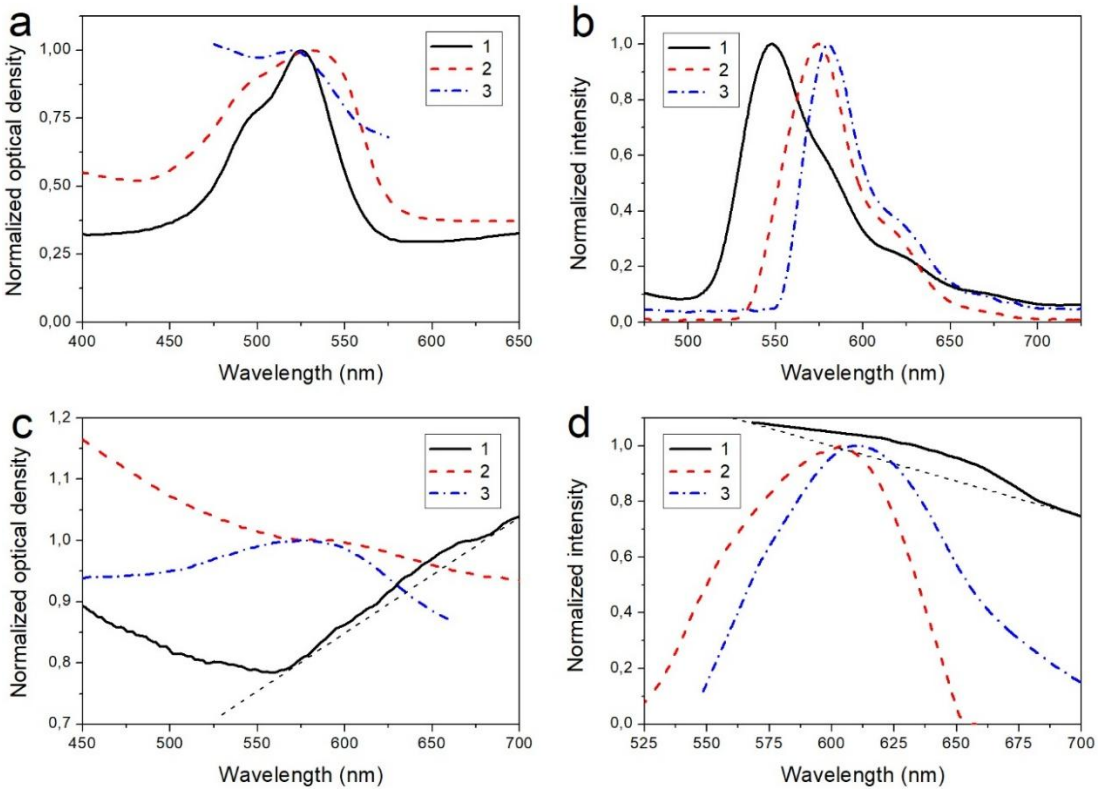

Fig. 4 – Absorption (a, c) and fluorescence (b, d) spectra of film samples normalized to the maximum values of the bands: 1 – PVA with dye/QDs, 2 – EVA and silica gel with dye/QDs, 3 – Aerosil with dye. (a, b) – R6G dye, (c, d) – NR dye

Table 1 – Positions of maxima of the absorption and fluorescence spectra of the films

Film sample	Absorption maximum, nm	Fluorescence maximum, nm
PVA with R6G/QDs	525	547
EVA and silica gel with R6G/QDs	530	574
Aerosil with R6G	523	581
PVA with NR/QDs	640-660	630-650
EVA and silica gel with NR/QDs	593-610	604
Aerosil with NR	576	610

In Aerosil films doped with NR, the electronic absorption spectrum changes upon adsorption of acetone molecules (Fig. 6). In clean air, the absorption band maximum is at 576 nm. When interacting with acetone molecules, a hypsochromic shift of the absorption band occurs, and the fluorescence intensity decreases (inset in Fig. 6). The magnitude of these changes was proportional to the concentration of acetone in the air. Thus, at 8000 ppm, the maximum was at 554 nm, and the shift relative to 0 ppm (clean air) was 22 nm. As the acetone concentration increases, the film optical density decreases from 0.374 for 0 ppm to 0.373 for 8000 ppm (at the band maximum). Also, when interacting with ammonia molecules, fluorescence quenching was observed in EVA with silica gel and PVA films functionalized with NR/QDs.

A typical fluorescence kinetics is shown in Fig. 7. For the first 120 seconds, the cuvette with the sample contained clean air. After 120-th second, an air sample with an analyte of a given concentration was pumped through. At this moment, analyte molecules began adsorbing onto the film's developed porous surface and interacting with immobilized dye molecules. As a result, fluorescence quenching occurred. When the adsorption and desorption rates reached dynamic equilibrium, the fluorescence intensity reached a steady level. It can be determined that the characteristic time of the decrease in fluorescence intensity during the adsorption of 40 ppm of acetone is 10 s.

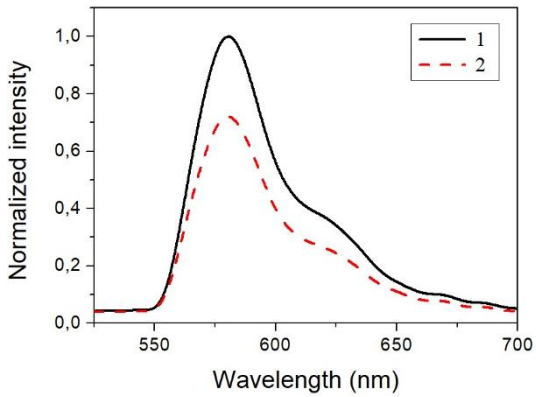

Fig. 5 – Fluorescence spectrum of an Aerosil film doped with R6G: 1 – in air without acetone; 2 – under adsorption of acetone molecules from air (concentration 400 ppm). Spectrum is normalized to the maximum value

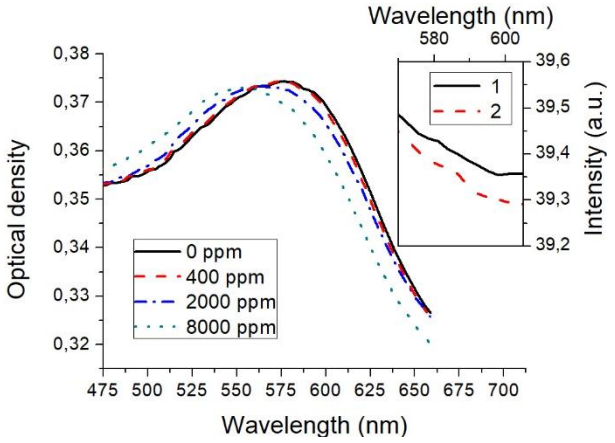

Fig. 6 – Absorption spectra of the Aerosil film doped with NR under the adsorption of different concentrations of acetone. The inset shows a fragment of the fluorescence excitation spectra of such a sample: 1 – in pure air, 2 – after adsorption of acetone molecules from the air at a concentration of 50 ppm

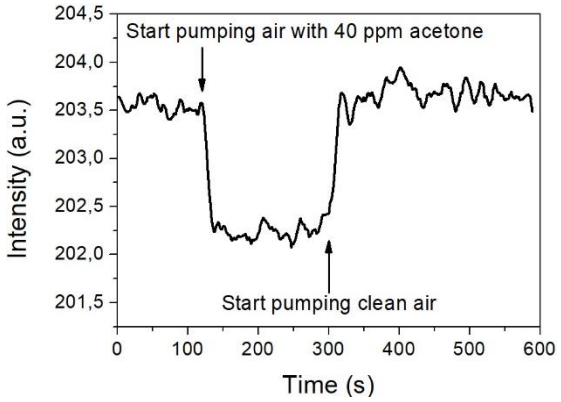

Fig. 7 – Fluorescence kinetics of an Aerosil film doped with NR: in the time interval 120-300 s – pumping air containing 40 ppm acetone, 0-120 s and 300-600 s – air without acetone

After 300-th second, when clean air began to flow through the cuvette containing the film, the analyte molecules were desorbed from the film's porous surface, and the fluorescence intensity gradually returned to its initial level. The restoration of fluorescence was almost complete with a characteristic time of about 11 s. The measurements were carried out with the air mixture recirculating in a closed container-cuvette circuit.

The diagram (Fig. 8) shows the relative changes in fluorescence intensity of the film samples upon exposure to trace concentrations (5 ppm) of the analytes in air.

$$\Delta I_r = \frac{I_0 - I}{I_0} \cdot 100\% \qquad (1)$$

These changes in percent ΔI_r were determined as the relative difference between the intensity in clean air I_0, i.e., before analyte adsorption, and the intensity in air with acetone or ammonia impurities after establishing a steady intensity value I, i.e., after analyte adsorption (see equation 1). The value ΔI_r was taken as a sensor response.

Possible explanation of fluorescence intensity changes in films with R6G is dynamic quenching by acetone via electron transfer from the quencher to the R6G molecule in the excited state [39]. It can also be assumed that similar mechanism explain the quenching of R6G by ammonia.

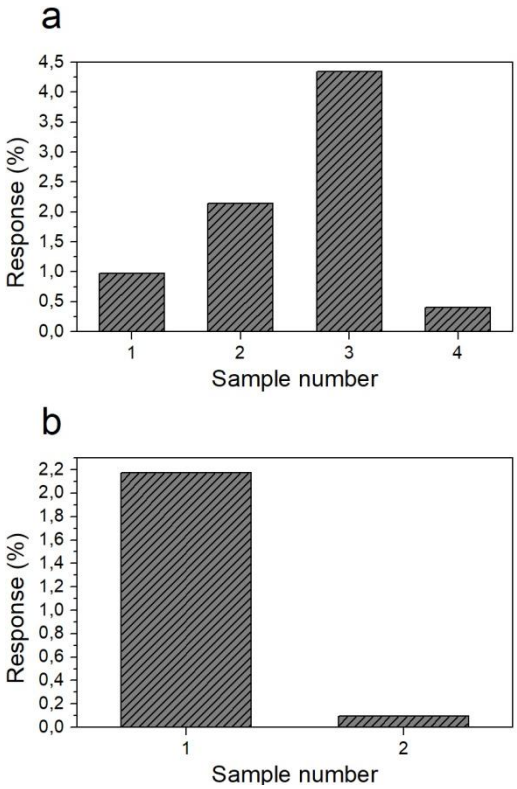

Fig. 8 – Sensor responses of film samples to analytes trace amounts in the air. (a) at 5 ppm ammonia: 1 – PVA with R6G/QDs, 2 – EVA and silica gel with R6G/QDs, 3 – PVA with NR/QDs, 4 – EVA and silica gel with NR/QDs. (b) at 5 ppm acetone: 1 – Aerosil with R6G, 2 – Aerosil with NR

Changes in the position of bands in the electronic absorption and fluorescence spectra of NR in films upon adsorption of polar molecules of acetone or ammonia are explained by the pronounced solvatofluorochromic properties of the dye – the dependence of the energy of electronic transitions on the polarity of the molecular environment [40]. The decrease in the fluorescence intensity of film samples upon adsorption of acetone or ammonia from the air is also associated with the significant dependence of this property of the dye on the environment's polarity [41].

4. CONCLUSIONS

New highly sensitive sensor composite films for detecting trace amounts of acetone and ammonia in the air have been studied, based on polyvinyl alcohol, Aerosil, or ethylene vinyl acetate with silica gel, with rhodamine 6G or Nile red dyes and their complexes with CdTe quantum dots. Selecting quantum dots of a specific size ensured the enhancement of the dye molecules' fluorescence via Förster resonance energy transfer, which increased sensor sensitivity by improving the signal-to-noise ratio. The sensor response is manifested by quenching of the fluorescence of rhodamine 6G and Nile red molecules. In samples containing Nile red, quenching is explained by the dye's pronounced

solvatofluorochromic properties, which result in a strong dependence of the spectral band's position and intensity on the polarity of the molecular environment. At the same time, the quenching mechanism of rhodamine 6G is not fully understood. To date, the materials studied allow us to detect ultra-low concentrations of acetone and ammonia in the air at levels no worse than 5 ppm. The sensors are characterized by almost complete recoverability, short response and recovery times (about 10 s for Aerosil films), and the possibility of repeated use. Such films could be applied to manufacture sensors for detecting acetone and ammonia in human exhaled air for rapid, non-invasive diagnosis or monitoring of diseases such as diabetes mellitus, renal failure, and lung cancer, especially due to their high sensitivity, ease of manufacture, and low cost.

ACKNOWLEDGMENTS

We acknowledge the financial support of the National Academy of Sciences of Ukraine (No. 0118U006321).

DECLARATION OF COMPETING INTEREST

The authors have no conflicts to disclose.

DATA AVAILABILITY

Data will be made available on request.

AUTHORSHIP CONTRIBUTION STATEMENT

Yaroslav Lazorenko and Vita Mitsai contributed equally to this work.

Yaroslav Lazorenko: Data curation (equal); Investigation (equal); Methodology (equal); Writing – original draft (equal); Conceptualization (equal); Visualization (equal). **Vita Mitsai:** Data curation (equal); Investigation (equal); Methodology (equal); Writing – original draft (equal); Conceptualization (equal); Visualization (equal). **Serhii Mamilov:** Project administration (equal); Supervision (equal); Writing – review & editing (equal). **Vladimir Sokolov:** Writing – review & editing (equal). **Vladimir Golub:** Supervision (equal).

REFERENCES

1. R. Selvaraj, N.J. Vasa, S.M.S. Nagendra, B. Mizaikoff, *Molecules* **25** No 9, 2227 (2020) https://doi.org/10.3390/molecules25092227.
2. V. Saasa, T. Malwela, M. Beukes, M. Mokgotho, C.-P. Liu, B. Mwakikunga, *Diagnostics* **8** No 1, 12 (2018) https://doi.org/10.3390%2Fdiagnostics8010012.
3. A. Abbaszadeh, S. Makouei, S. Meshgini, *Photonics Nanostructures: Fundam. Appl.* **44**, 100917 (2021) https://doi.org/10.1016/j.photonics.2021.100917.
4. Y. Qi, W. Xu, N. Ding, X. Chang, C. Shang, H. Peng, T. Liu, Y. Fang, *Mater. Chem. Front.* **3**, 1218 (2019) https://doi.org/10.1039/C9QM00095J.
5. G. Song, D. Jiang, J. Wu, X. Sun, M. Deng, L. Wang, C. Hao, J. Shi, H. Liu, Y. Tian, M. Chen, *Chem. Eng. J.* **440**, 135979 (2022) https://doi.org/10.1016/j.cej.2022.135979.
6. M. Alshareef, R.M. Snari, O. Alaysuy, A.M. Aldawsari, H.M. Abumelha, H. Katouah, N.M. El-Metwaly, *ACS Omega* **7** No 19, 16766 (2022) https://doi.org/10.1021/acsomega.2c01492.
7. V.P. Mitsai, V.O. Golub, *Ukr. J. Phys.* **70** No 7, 442 (2025) https://doi.org/10.15407/ujpe70.7.442.
8. Ya.P. Lazorenko, V.O. Sokolov, S.V. Kryvets, S.O. Mamilov, *Ukr. J. Phys.* **70** No 4, 237 (2025) https://doi.org/10.15407/ujpe70.4.237.
9. R. Sobczyk, L. Galmiche, C. Mongin, M. Djendli, I. Leray, R. Méallet, *Photochem. Photobiol. Sci.* **24**, 165 (2025) https://doi.org/10.1007/s43630-025-00681-3.
10. S. Majumder, S. Deb, S. Hussain, D. Dey, D. Bhattacharjee, A.N. Alodhayb, S. Hussain, S.A. Hussain, *Sci. Rep.* **15**, 2824 (2025) https://doi.org/10.1038/s41598-024-84846-7.
11. V.P. Mitsai, Ya.P. Lazorenko, A.G. Misyura, S.O. Mamilov, *Nanosist. nanomater. nanotehnol.* **19** No 4, 941 (2021) https://doi.org/10.15407/nnn.19.04.941.
12. V.P. Mitsai, A.G. Misyura, S.V. Kryvets, Ya.P. Lazorenko, *J. Nano- Electron. Phys.* **8** No 4, 04032 (2016) https://doi.org/10.21272/jnep.8(4(1)).04032.
13. S. Jung, X. Chen, *Adv. Healthc. Mater.* **7** No 14, e1800252 (2018) https://doi.org/10.1002/adhm.201800252.
14. H.B. Chandrasiri, H. Jing, T. Perera, Y.S. Hu, P.T. Snee, *J. Phys. Chem. Lett.* **14** No 15, 3621 (2023) https://doi.org/10.1021/acs.jpclett.3c00076.
15. S. Park, J.-C. Vial, K. Kyhm, *Opt. Express* **25**, 18917 (2017) http://doi.org/10.1364/OE.25.018917.
16. P.C. Beaumont, D.G. Johnson, B.J. Parsons, *J. Chem. Soc. Faraday Trans.* **89**, 4185 (1993) https://doi.org/10.1039/FT9938904185.
17. Y. Fang, J. Hu, C. Huang, *Opt. Commun.* **549**, 129889 (2023) https://doi.org/10.1016/j.optcom.2023.129889.
18. Y. Fang, J. Cheng, G. Wang, T. Dong, S. Wang, C. Gu, G. Zou, H. Ming, L. Xu, *Appl. Opt.* **58** No 16, 4345 (2019) https://doi.org/10.1364/AO.58.004345.
19. A. Ogunsipe, *J. Solut. Chem.* **47**, 203 (2018) https://doi.org/10.1007/s10953-017-0706-8.
20. H. Tajalli, A.G. Gilani, M.S. Zakerhamidi, P. Tajalli, *Dyes Pigm.* **78** No 1, 15 (2008) https://doi.org/10.1016/j.dyepig.2007.10.002.
21. Z. Zhang, R. Han, S. Chen, F. Zheng, X. Ma, M. Pan, S. Wang, *Foods* **12** No 5, 1085 (2023) https://doi.org/10.3390/foods12051085.
22. J. Mandal, P. Ghorai, K. Pal, T. Bhaumik, P. Karmakar, A. Saha, *ACS Omega* **5** No 1, 145 (2020) https://doi.org/10.1021/acsomega.9b02181.
23. C. Preininger, G.J. Mohr, I. Klimant, O.S. Wolfbeis, *Anal. Chim. Acta* **334** No 1-2, 113 (1996) https://doi.org/10.1016/S0003-2670(96)00269-3.
24. F. Mohammadzadeh, M. Golshan, V. Haddadi-Asl, M. Salami-Kalajahi, *Sens. Actuators A: Phys.* **379**, 115933 (2024) https://doi.org/10.1016/j.sna.2024.115933.
25. C. Gajo, D. Shchepanovska, J.F. Jones, G. Karras, P. Malakar, G.M. Greetham, O.A. Hawkins, C.J.C. Jordan, B.F.E. Curchod, T.A.A. Oliver, *J. Phys. Chem. B* **128** No 47, 11768 (2024) https://doi.org/10.1021/acs.jpcb.4c06048.
26. S. Prasad, A. Bennett, M. Triantafyllou, *J. Mar. Sci. Eng.* **12** No 8, 1403 (2024) https://doi.org/10.3390/jmse12081403.
27. L. Sessa, S. Concilio, M.D. Martino, A.M. Nardiello, Y. Miele, F. Rossi, J. Brunetti, B. Panunzi, S. Piotto, *Dyes Pigm.* **196**, 109759 (2021) https://doi.org/10.1016/j.dyepig.2021.109759.
28. X. Rong, Z.-Y. Xu, J.-W. Yan, Z.-Z. Meng, B. Zhu, L. Zhang, *Molecules* **25** No 20, 4718 (2020) https://doi.org/10.3390/molecules25204718.
29. J.-Y. Lv, M.A.H. Nawaz, N. Liu, H.-P. Zhou, E. Hussain, X. Wen, X.-Y. Gou, X. Jin, C. Yu, *Chin. J. Anal. Chem.* **50** No 9, 100140 (2022) https://doi.org/10.1016/j.cjac.2022.100140.
30. D. Liu, X. Lian, A.K. Mallik, W. Han, F. Wei, J. Yuan,

C. Yu, G. Farrell, Y. Semenova, Q. Wu, *25th International Conference on Optical Fiber Sensors (OFS-25)* 103232W, 103232W-1 (Proc. SPIE 10323: 2017) https://doi.org/10.1117/12.2263671.
31. S. Nguyen, Z.J. Delalic, D.M. Kargbo, J.B. Sheffield, *IMAPSource Proc.* **2012** No 1, 1185 (2012) https://doi.org/10.4071/isom-2012-THP53.
32. S. Che, A. Xu, J. Zou, S. Luo, X. Peng, H. Fu, Y. She, *Food Res. Int.* **209**, 116233 (2025) https://doi.org/10.1016/j.foodres.2025.116233.
33. S. Czihal, F. Bauer, M. Bertmer, A. Kahnt, S. Naumov, M. Lau, D. Enke, *RSC Appl. Interfaces* **2** No 4, 995 (2025) https://doi.org/10.1039/D5LF00060B.
34. M. Gerboles, E. Diaz, A. Noriega-Guerra, *Accredit. Qual. Assur.* **3**, 69 (1998) https://doi.org/10.1007/s007690050188.
35. M. Chapman, W.B. Euler, *J. Fluoresc.* **28**, 1431 (2018) https://doi.org/10.1007/s10895-018-2318-0.
36. I.T. Sugiarto, Isnaeni, K.Y. Putri, "Analysis of dual peak emission from Rhodamine 6G organic dyes using photolminescence," *J. Phys.: Conf. Ser.* **817**, 012047 (2017) https://doi.org/10.1088/1742-6596/817/1/012047.
37. A. Minò, G. Cinelli, F. Lopez, L. Ambrosone, *Appl. Sci.* **13** No 1, 638 (2023) https://doi.org/10.3390/app13010638.
38. C.A. Guido, B. Mennucci, D. Jacqueminc, C. Adamo, *Phys. Chem. Chem. Phys.* **2**, 8016 (2010) https://doi.org/10.1039/B927489H.
39. M.C. Palazzotto, M.R.V. Sahyun, N. Serpone, D.K. Sharma, *J. Chem. Phys.* **90**, 3373 (1989) https://doi.org/10.1063/1.455891.
40. M. Hornum, P. Reinholdt, J.K. Zarę ba, B.B. Jensen, D. Wüstner, M. Samoć, P. Nielsen, J. Kongsted, *Photochem. Photobiol. Sci.* **19**, 1382 (2020) https://doi.org/10.1039/d0pp00076k.
41. L. Lacerda, H. Ali-Boucetta, S. Kraszewski, M. Tarek, M. Prato, C. Ramseyer, K. Kostarelos, A. Bianco, *Nanoscale* **5** No 21, 10242 (2013) https://doi.org/10.1039/C3NR03184E.

Пористі плівки з родаміном 6Ж, нільським червоним та квантовими точками CdTe для високочутливого виявлення ацетону та аміаку в повітрі

Я.П. Лазоренко[1,2], В.П. Міцай[2], С.О. Мамілов[2], В.О. Соколов[2], В.О. Голуб[2]

[1] *Інститут металофізики ім. Г.В. Курдюмова НАН України, 03142 Київ, Україна*
[2] *Інститут магнетизму ім. В.Г. Бар'яхтара НАН України, 03142 Київ, Україна*

Виявлення молекул в низьких концентраціях у багатокомпонентному газовому середовищі є складною задачею. Хоч наразі досліджуються та розробляються різні сенсори, вони не завжди відповідають вимогам високої чутливості, селективності, роботи при кімнатній температурі та низької собівартості. Одним з перспективних підходів в цьому аспекті є флуоресцентні плівкові сенсори. Метою цього дослідження було вивчити оптичні властивості та флуоресцентні сенсорні відгуки пористих плівок, допованих родаміном 6Ж або Нільським червоним, або їх комплексами з квантовими точками CdTe. Плівкові матриці складалися з полівінілового спирту, аеросилу (пірогенного кремнезему) або етиленвінілацетату з силікагелем. Квантові точки вводились для посилення сигналу флуоресценції за рахунок безвипромінювального Ферстерівського резонансного переносу енергії. Отримано спектри оптичного поглинання та флуоресценції плівок у видимій області. Зниження інтенсивності флуоресценції відповідало концентрації аналіту. Виявлено сенсорні відгуки на низькі концентрації аміаку або ацетону (5 ppm). Найвищу чутливість до ацетону та аміаку продемонстрували плівки аеросилу, доповані родаміном 6Ж, та полівінілового спирту, доповані Нільським червоним з квантовими точками CdTe розміром 2,9 нм, відповідно. Така висока чутливість спостерігалась за кімнатної температури. На основі експериментальних результатів та унікальних властивостей матеріалів зроблено висновок, що такі плівки можуть бути використані як чутливі елементи сенсорів для неінвазивної діагностики захворювань шляхом виявлення концентрацій біомаркерів у видихуваному повітрі або для моніторингу навколишнього середовища.

Ключові слова: Сенсор, Флуоресцентні барвники, Родамін 6Ж, Нільський червоний, Ацетон, Аміак, Флуоресценція, Квантові точки.